INDIAN JOURNAL OF SCIENCE AND TECHNOLOGY

RESEARCH ARTICLE

Fractal and Time-series A nalyses based Rhonchi and Bronchial Auscultation: A Machine Learning Approach

Ammini Renjini[1], Mohanachandran Nair Sindhu Swapna[1], Vimal Raj[1], Sankararaman Sreejyothi[2], Sankaranarayana Iyer Sankararaman[1]*

1 Department of Optoelectronics, University of Kerala, Trivandrum, 695581, Kerala, India
2 Former intern, Department of Optoelectronics, University of Kerala, Trivandrum, 695581, Kerala, India

OPEN ACCESS

Received: 19-03-2022
Accepted: 01-05-2022
Published: 21-06-2022

Citation: Renjini A, Sindhu Swapna MN, Raj V, Sreejyothi S, Sankararaman SI (2022) Fractal and Time-series A nalyses based Rhonchi and Bronchial Auscultation: A Machine Learning Approach. Indian Journal of Science and Technology 15(21): 1041-1051. https://doi.org/10.17485/IJST/v15i21.627

* **Corresponding author**.

drssraman@gmail.com

Funding: None

Competing Interests: None

Published By Indian Society for Education and Environment (iSee)

ISSN
Print: 0974-6846
Electronic: 0974-5645

Abstract

Objectives: The present work reports the study of 34 rhonchi (RB) and Bronchial Breath (BB) signals employing machine learning techniques, time-frequency, fractal, and non-linear time-series analyses. **Methods:** The time-frequency analyses and the complexity in the dynamics of airflow in BB and RB are studied using both Power Spectral Density (PSD) features and non-linear measures. For accurate prediction of these signals, PSD and non-linear measures are fed as input attributes to various machine learning models. **Findings:** The spectral analyses reveal fewer, low-intensity frequency components along with its overtones in the intermittent and rapidly damping RB signal. The complexity in the dynamics of airflow in BB and RB is investigated through the fractal dimension, Hurst exponent, phase portrait, maximal Lyapunov exponent, and sample entropy values. The greater value of entropy for the RB signal provides an insight into the internal morphology of the airways containing mucous and other obstructions. The Principal Component Analysis (PCA) employs PSD features, and Linear Discriminant Analysis (LDA) along with Pattern Recognition Neural Network (PRNN) uses non-linear measures for predicting BB and RB. Signal classification based on phase portrait features evaluates the multidimensional aspects of signal intensities, whereas that based on PSD features considers mere signal intensities. The principal components in PCA cover about 86.5% of the overall variance of the data class, successfully distinguishing BB and RB signals. LDA and PRNN that use non-linear time-series parameters identify and predict RB and BB signals with 100% accuracy, sensitivity, specificity, and precision. **Novelty:** The study divulges the potential of non-linear measures and PSD features in classifying these signals enabling its application to be extended for low-cost, non-invasive COVID-19 detection and real-time health monitoring.

Keywords: lung signal; fractal analysis; sample entropy; nonlinear timeseries; machine learning techniques

1 Introduction

Respiratory diseases kill almost 3 million people each year, making them one of the leading causes of pulmonary illness and fatalities. The World Health Organization divulges that Chronic Obstructive Pulmonary Disease (COPD) takes over the third position in causing death in First World countries. The primary procedure for diagnosing lung conditions by physicians is auscultation. The airflow through the respiratory tract produces lung sounds and gives valuable information about the lung condition, diseases, and obstructions in the airways. Breath sounds are commonly divided into two categories - normal and adventitious [1]. Over the bronchi, basis pulmonis, and lung periphery, normal breath sounds such as bronchial (BB), vesicular, and bronchovesicular are auscultated. Rhonchi (RB), crackle, wheeze, stridor, and pleural rub are examples of adventitious breath sounds that identify acquired lung diseases such as restriction in large airways, fluid accumulation in or around lungs, air passage constriction leading to inflation of a portion of the lungs, pleural layer inflammation, and others [2]. The pitch of the breath sound and the ratio of inspiration to expiration duration vary depending on where it originates. As a result, a thorough diagnosis of lung disorders requires an inquiry to determine the hallmark characteristics of normal and abnormal sounds. The paper focuses on the study of rhonchi breath sound reflecting the pathological conditions of the lung.

Rhonchi is a continuous, low-pitched, adventitious lung sound that is heard in bronchi during both the inspiratory and expiratory lung cycle [3], which indicates COPD, pneumonia, bronchiectasis, and bronchitis [4,5]. For auscultation and biomedical imaging, several mathematical tools like Fourier transform and wavelet transform have been employed [6]. These techniques help in transforming the auscultation signal in the time domain to the frequency domain. The frequency components present in the normal and adventitious breath signals vary depending on their origin and the diameter of airways [7]. Though the Fourier transform can tell us the frequency components and their intensities, it is unable to provide details regarding the instance of its occurrence [8]. The wavelet transform, which brings out the temporal information, overcomes this limitation by providing the time and duration of occurrence of a particular frequency component together with its intensity. The sound due to the airflow through the respiratory tract is a time-series data reflecting the lung condition. The non-linear time-series analysis of the signal gives information about the respiratory tract conditions besides the lung condition.

Non-linear time-series analysis is a potent mathematical technique to unveil the deterministic and stochastic parameters of time-series data. Geometric representation of the complex trajectories of a dynamic system could be represented by its phase portrait drawn in the two-dimensional phase space. The construction of the phase portrait, and the maximal Lyapunov exponent (λ), point to the complexity of a system [9]. The Fractal dimension (D) [10], Hurst exponent (H), and sample entropy (S) are regarded as the measures of complexity and randomness of a system. Several methods like epsilon-blanket, walker-divider, power spectrum, and box-counting methods are used for finding fractal dimension depending on the nature of the problem. The sample entropy, a parameter proposed by J. S. Richman, E. Lake, and J. R. Moorman, describes the system's complex, uncertain, and random nature, which measures the speediness of the information generated in the time-series and is widely employed in biomedical engineering [11].

Computer-based unsupervised and supervised classifiers help automatically classify lung sounds in real-time. Data sets with identical characteristics can be classified with the unsupervised principal component analysis (PCA) based on dimensionality reduction. Supervised learning models - linear discriminant analysis (LDA) and pattern

recognition neural network (PRNN) provide precise classification and prediction of breath sound based on the extracted features. The multidimensional aspects of dynamic non-stationary time-series lung sound like complexity, randomness, and unpredictability can be efficaciously evaluated by analyzing the non-linear features of the signal. The present work inquires about the adventitious breath sound rhonchi through machine learning techniques, time-frequency, non-linear time-series, and fractal analyses and compares it with the normal breath signal BB to explore the possibility of employing them in lung auscultation for efficient classification with a higher prediction accuracy rate.

2 Materials and Methods

In the present study, thirty-four lung sound signals gathered from online databases with a duration of 2 s – 5 s at a sampling frequency of 44,100 Hz [12–14] are subjected to frequency domain/fast Fourier transform, time-frequency localization/wavelet, and non-linear time-series analyses. For classifying the normal and pathological sound signals, the feature extraction method is adopted for PCA. The BB and RB sound signals in the time domain (t) are transformed into the frequency domain (ω) by the fast Fourier transform technique for carrying out the analysis. The signal's ($x(t)$) Fourier transform, $X(\omega)$ is calculated as [15],

$$X(\omega) = \int x(t) e^{-j\omega t} dt. \quad (1)$$

The PSD function, which provides the signal power (P) distribution over a specific range of frequency (f), can be computed from the fast Fourier transform signal of length N by [15],

$$P = \frac{(X(f)|^2}{N}. \quad (2)$$

The PSD function gives the signature frequency components of the signal that can be used in feature extraction for classifying the signals by the unsupervised machine learning classifier, PCA. For this, the data in the range 100 Hz – 1000 Hz is divided into twenty-six sub-bands, and the average value of P for each sub-band is taken as the representative feature for performing PCA using R programming.

The temporal distribution of frequency components with their intensities can be obtained from the wavelet analysis. Morse wavelets are eigenfunction wavelets that may be used to estimate time-varying spectral bands by taking the average of time-scale Eigen scalograms. They are suitable for examining real signals, which have varying amplitude and frequency over time and are employed to investigate localized discontinuities as well. Thus the translation of the mother wavelet – Morse wavelet (φ)-through the signal generates the wavelets useful for the analysis of the signal. The wavelet transform of the signal $x(t)$ for a scale parameter ε and translation parameter γ is given by [16],

$$W_c f(\varepsilon, \gamma) = \int_{-\infty}^{\infty} x(t) . \varepsilon^{-1/2} \varphi\left(\frac{t-\gamma}{\varepsilon}\right) dt. \quad (3)$$

Non-linear signals that are continuous in time but non-stationary are either periodic or non-periodic. A non-linear time-series study provides information about the underlying parameter values of the data set. Applying Cao's algorithm, the phase portrait is plotted using the parameters - embedding dimension (m) and the time delay (τ) (found out from the mutual information function). The reconstructed vector X of length n in the phase space is [8],

$$X = X_{n-(m-1)\tau}, X_{n-(m-2)\tau}, \ldots\ldots, X_n. \quad (4)$$

As the system evolves in time, the Maximal Lyapunov exponent (λ) quantifies the probable average separation between neighboring state-space orbits/curves. A positive λ indicates the exponential divergence of the system with time, suggesting randomness and unpredictability. The distance between two Takens' vectors in the phase space δ(t) and δ(0) at time t and t = 0 are related by,

$$log \frac{\delta(t)}{\delta(0)} = \lambda \cdot t. \quad (5)$$

The slope in equation (5) estimates λ [8].

To estimate the time-series data's complexity, one can employ the parameters – D, H, and S. D is a measure showing that the patterns in a time-series are self-affine. The box-counting technique estimates the value of D by placing the signal on grids of different dimensions, 's,' and counting the number of grids N(s) necessary to cover the signal. N(s) and s possess values that obey a fractal power law with D, given by [10],

$$N(s) \propto s^{-D}.$$

The value of D is the slope of $logN(s)$ vs. $log\left(\frac{1}{s}\right)$ graph from which H value can be estimated as [8],

$$H = 2 - D.$$

It represents the long-term memory of a time-series, and its value ranges from 0 to 1. The value of H classifies the time-series into – (i) antipersistent (when H lies between 0 and 0.5), (ii) Brownian (when H = 0.5), and persistent (when H lies between 0.5 and 1) [17].

The measure of randomness in a data may be assessed from sample entropy [18] $S(m,r)$ derived from the correlation sum C (r) of dimensions m and m+1 for a radius r as given in Eq. (8). The mean sample entropy for multiple r values is the sample entropy value at a certain embedding dimension [19].

$$S(m,r) = ln\left(\frac{C^m(r)}{C^{m+1}(r)}\right). \quad (8)$$

The non-linear time-series features - S, λ, m, D, and τ - give significant information about the multidimensional characteristics of a lung sound signal. Supervised learning models – LDA and PRNN – based on non-linear features are employed to classify and predict BB and RB, where seventy percent of the total data set is subjected to five-fold cross-validation for model training, and the remaining for signal prediction. To assess classification performance, the confusion matrix (CM) and the Area Under the Receiver Operating Characteristic (ROC) Curve (AUC) are utilized [20]. As the accuracy of the trained model increases, prediction accuracy also increases. Machine learning models predict the sample data into four categories, and the associated terminologies obtained from a CM are - (i) True-positive (TP), (ii) False-positive (FP), (iii) True-negative (TN), and (iv) False-negative (FN). Based on these metrics from the CM, various statistical parameters - accuracy, sensitivity, specificity, and precision - are defined to assess supervised learning models' performance [20]. The LDA and PRNN are performed with the help of the 'Classification learner ' and 'nprtool,' respectively, in the MATLAB R2020a to classify and predict BB and RB signals.

3 Results and Discussions

The study detailed in the paper suggests a new method for auscultation employing mathematical techniques. The BB and RB being a time-series, as shown in Figure 1, the signals are analyzed using spectral and time-series analyses for diagnosing the lung condition. The analysis helps in unveiling the characteristic features in the breath sound signals corresponding to a particular pathological condition. Of the thirty-four samples analyzed, a representative time spectrum of BB and RB is shown in Figure 1, whose fast Fourier transform is depicted in Figure 2. From Figure 1, it is oberved that the bronchial breath takes about 2.5 s to complete one respiration, while the RB showing the pathological state of the lung, completes one respiration in 5 s. When BB displays a pause between the two phases of respiration, the RB signal exhibits a near continuity with lesser sound intensity. The origin of the BB signal is due to the flow of air through the bronchi and trachea [6]. From Figure 1, it can also be understood that the inspiration and expiration in BB have almost the same loudness compared to the lesser sound intensity during expiration in RB. The lowering of sound intensity in RB can be understood from its origin. The obstructions or increased fluid secretions in bronchi cause turbulence in the air passing through it, generating the RB signal. The airflow through obstructions and fluid secretions results in the damping of the amplitude of vibration of the air molecules producing the sound signal, as shown in the inlay of Figure 1b. The chain of rapidly damped sinusoidal oscillations, shown in the inlay figure of Figure 1b, is the magnified image of a portion of the signal, which is the characteristic of RB. The reduction of loudness can also be viewed as the energy dissipation of the moving air molecules on collision with the soft fluid media between the airways and the bronchi wall.

The fast Fourier transform analysis of RB and BB sound signals, shown in Figure 2a and 2b reveal that RB shows a lesser number of frequency components of lower intensities than BB. A closer examination of the PSD plot of RB shows overtone bands in the region 430 Hz – 600 Hz corresponding to the fundamental frequency components in the region 215 Hz – 300 Hz. In addition to the absence of the overtone band in BB, the center frequency of the fundamental band shows a hypsochromic shift when compared with that of RB. The frequency spread in RB and BB decreases due to the narrowing of the bronchial tube caused by the presence of secretions and obstructions.

The lowering of frequency spread in RB than in BB is due to the lowering of the diameter of the bronchi caused by the presence of secretions and obstructions. The details displayed in the PSD plot (Figure 2a and 2b can be represented in the wavelet scalogram (Figure 2c and 2d), eliciting the time-instance of the occurrence of component frequencies along with their magnitudes. From the wavelet scalogram of BB (Figure 2c), it is evident that the period of occurrence of high-intense frequency components is longer all through BB inspiration than during expiration. It is interesting to note from Figure 2d that, albeit the high-intense frequency components are present, it lasts only for a short duration. The presence of overtone bands in Figure 2b, in addition to the fundamental, suggests that the diameter of the airways changes due to obstructions. The wavelet scalogram of RB displays its characteristic features like longer duration of breathing, lesser frequency spread, and the train of intermittent damping oscillations.

The airflow passing in and out through the thoracic cavity is a complex dynamic process that could be analyzed with a non-linear approach by plotting the phase portraits of both BB and RB signals shown in Figure 3a and 3b, using R programming. The optimal delay time is chosen as the time delay at which the average mutual information holds the smallest value, and the algorithm proposed by Cao estimates the embedding dimension. The λ values for bronchial and rhonchi lung sounds shown in the box plot (Figure 3c) display information about the rate at which the phase points diverge in time (with τ= 39 for BB and τ= 36 for RB), revealing the variation in the complexity depicted through the phase portraits (Figure 3a and 3b).

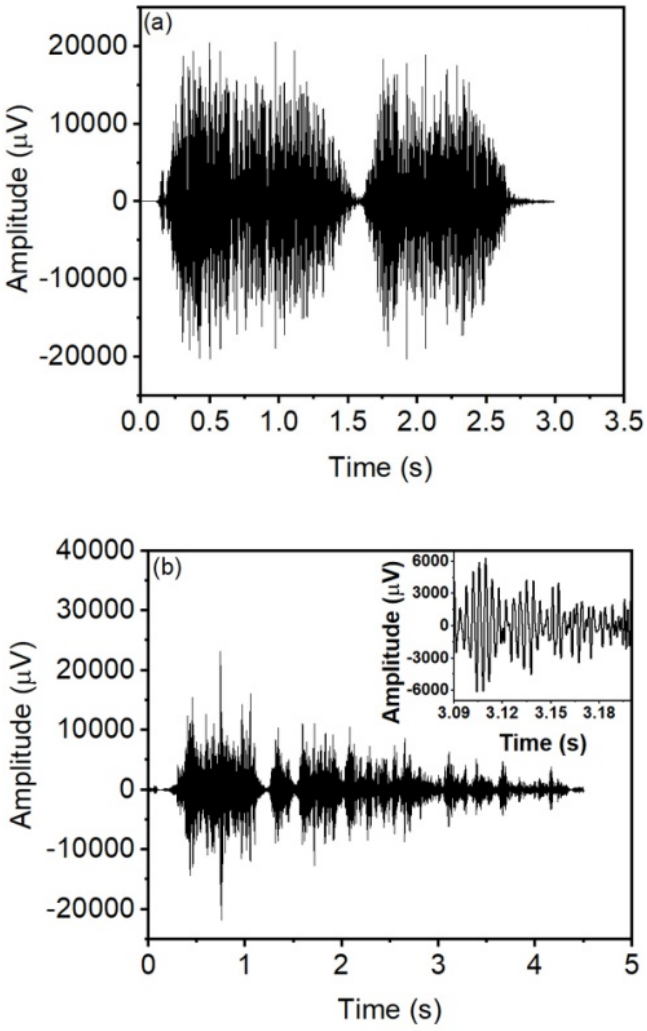

Fig 1. Time domain of lung sounds - (a) BB (b) RB.

Sample entropy (S) is another factor that determines the system's complexity. The value of the mean sample entropy for BB and RB represented through the box plot Figure 4a are 1.17 and 2.13, respectively. The higher value of entropy for the RB signal gives information not only about the increased complexity in the dynamics of airflow through the airways but also about the internal morphology of the airways containing mucus and other obstructions. The mucosal secretions and obstructions present non-uniformly changes the cross-sectional diameter of the airways different at different points. When the air flows through such an airway, vortices and turbulence gets generated, as represented in Figure 4b, resulting in a higher entropy value for RB.

The complexity of a self-affine signal is reflected through its fractal dimension, D. Figure 5a displays the box-whisker plot of D calculated for BB and RB lung sounds. It is found that the average value of D is less for RB than BB. The BB signal possesses larger complexity than the RB signal due to the persistence of high-intense multiple frequency components during respiration, as depicted in Figure 2 by the spectral density and wavelet analyses. Hurst exponent (H) is an important factor usually used for reflecting the complexity of a system represented as a time-series. The mean H values for RB and BB, shown in the box plot Figure 5b, are 0.27 and 0.198, respectively. An H value lying between 0 and 0.5 shows the negative correlation nature of the time-series, indicating the randomness involved in the airflow through the tracheobronchial tract. A value of H closer to 0.5 means more is the randomness associated with the signal, which attributes to the higher value of the same to the RB signal.

Artificial intelligence and deep convolutional neural networks have been employed to classify lung sounds using various input attributes such as spectral features (short-time Fourier transform, fast Fourier transform), cepstral features (Mel

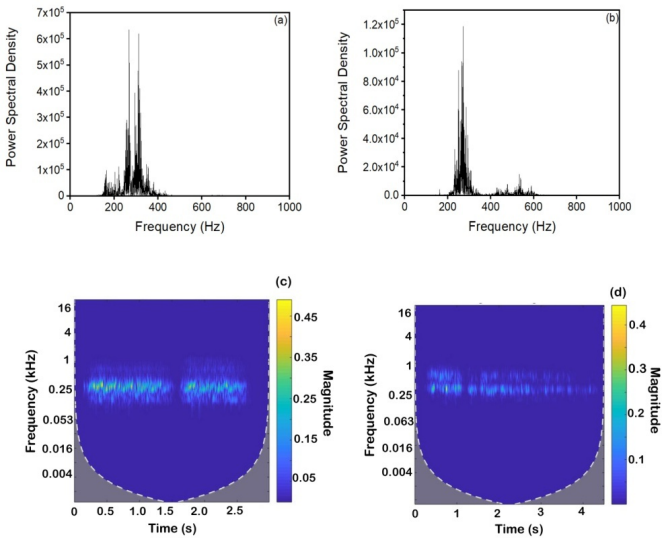

Fig 2. PSD plots of (a) BB signal (b) RB signal; Wavelet scalograms of (c) BB signal (d) RB signal.

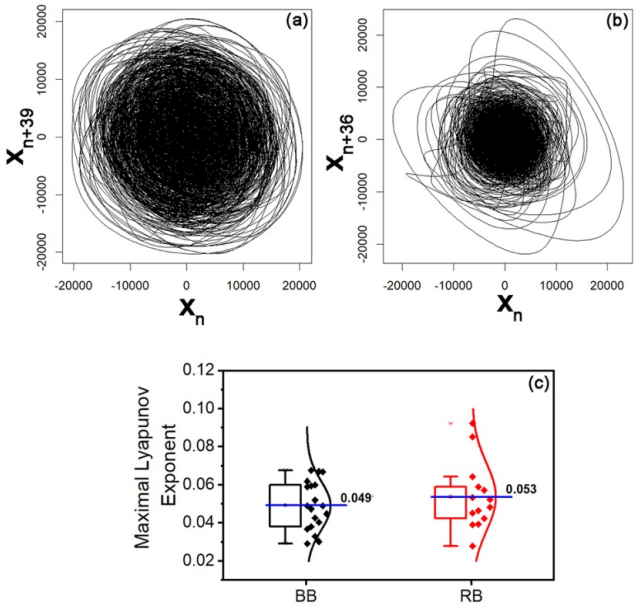

Fig 3. Phase portraits of the signals (a) BB, (b) RB, and (c) the box plot of maximal Lyapunov exponent for BB and RB.

coefficients), and a combination of both. A study carried out by Shin-Yun Jung et al.[(1)] provides a feature engineering technique for extracting specific features for the depth-wise separable convolution neural network (DS-CNN) to accurately and efficiently categorize lung sounds. The input features employed are the spectral (short-time Fourier-transform), the cepstral (Mel-frequency cepstrum coefficient), and the combined features of these two achieving an accuracy of 82.07%, 73.02%, and 85.74%, respectively. The VGG16 classifier employed by Yoonjoo et al. in CNN and support vector machine architectures classifies adventitious breath sounds - crackles, wheezes, or rhonchi - with an accuracy of 85.7% and an average AUC of 0.92[(5)]. Ravi Pal and Anna Barney employ an iterative envelope filter combined with a mean D value, which is capable of detecting synthesized fine and coarse crackles (except for real fine and coarse crackles)[(6)]. A CNN architecture implemented in Python using Keras has been employed by Baghel et al. to classify normal and one of the adventitious lung sounds (crepitation, rhonchi,

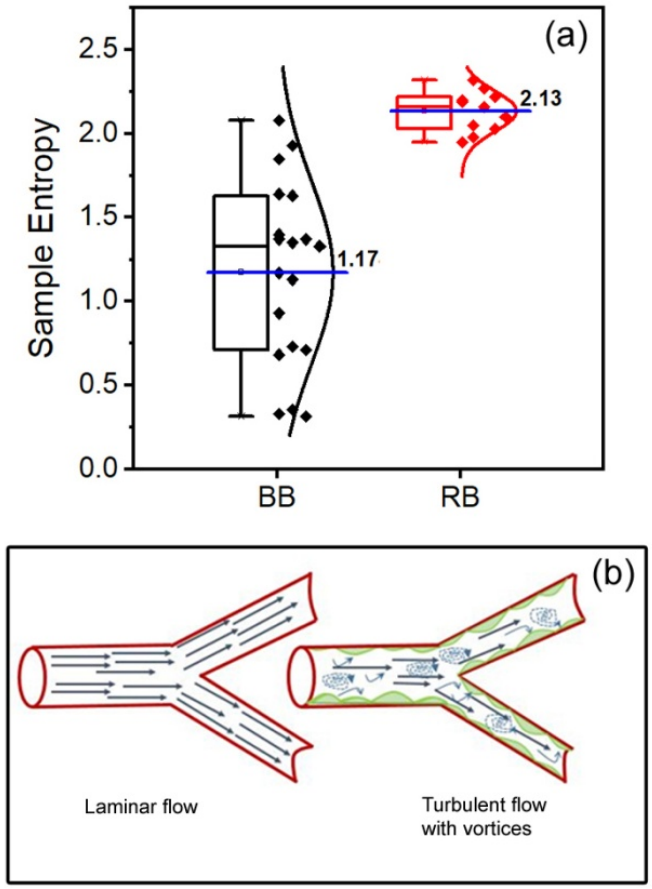

Fig 4. (a) Box plot of Sample Entropy of BB and RB and (b) Schematic of vortices and turbulence in airways.

and wheeze). An average validation accuracy of 94.24 % with a validation loss of 0.4859 is obtained with 958 and 106 training and validation samples[21].

PCA helps in distinguishing two data sets having similar parameters based on the method of feature extraction[22]. The signature frequency components of BB and RB appearing in the PSD are extracted by dividing the data sets into 26 sub-bands and taking the mean of each sub-band as its representative feature. The 26 features of each signal are taken to figure out the PCA using R studio software. The sum of the variances of all individual principal components is termed total variance, and the ratio of the variance of a principal component to the overall variance is the proportion of variance shown by that principal component. Thus the overall variance is the sum of the variances of all individual classes. The variance depicted by each individual class, when divided by the total variance, details how much variance each class of data explains. Here, when the variable classes (BB and RB) are combined, total variance of 86.5 % is obtained by taking the sum of variances of the first two principal components. The data classes are projected in the first two principal components in Figure 6, which cover about 86.5% of the total variance of the original data classes. This proves the potentiality of using PCA as a useful tool for the classification of BB and RB depending on their spectral characteristics.

Since PCA is an unsupervised learning method, supervised learning techniques, LDA and PRNN, are used to classify BB and RB. LDA classifies by increasing the variance between the groups and decreasing the variance within the group[23]. The phase portrait features S, λ, m, D, and τ, resulting from the non-linear time-series study of BB and RB, are the five attributes used to classify the signals as these parameters reflect the signal strength in addition to the temporal correlation. To achieve a balance between underfitting and overfitting, the hyperparameter tuning procedure is required. So seventy percent of the total number of breath sound signals used to train the network are subjected to five-fold cross-validation, which prevents the trainer LDA model from overfitting and increases the prediction accuracy.

The confusion matrix and the AUC of the classifier are shown in Figure 7. Figure 7a shows that the trained LDA model classifies BB and RB with 100% accuracy, and the AUC shown in Figure 7b depicts a value of 1, indicating its superior

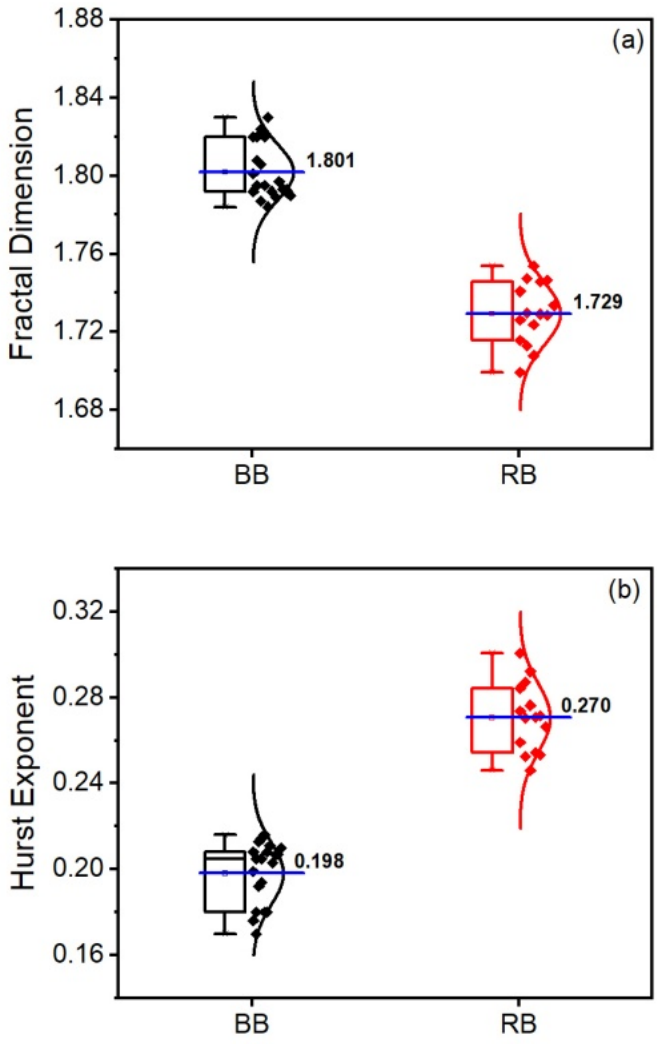

Fig 5. Box plots of the BB and RB signals (a) Fractal Dimension (b) Hurst exponent.

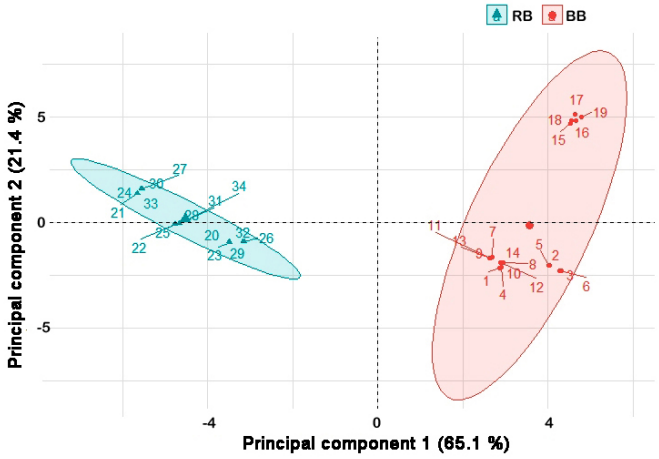

Fig 6. PCA of BB and RB signals.

classification ability. The specificity, sensitivity, and precision are also found to be 100%. Neural networks are a subclass of machine learning techniques and are the heart of deep learning algorithms. PRNN helps in classifying two datasets by discovering the regularity patterns in them with the help of dedicated algorithms[24]. A simple shallow neural network is constructed with a double-layer feed-forward network with five non-linear measures as input predictors and ten neurons in the second/hidden layer (Figure 8). The scaled conjugate gradient backpropagation technique is used to train the model with seventy percent data for training and thirty percent equally divided for testing/validation. For PRNN, the input dataset of BB and RB is divided into three categories – train data, test data, and validation data - in the percentage ratio of 70:15:15. The confusion matrices and the ROC curves of train, test, validation, and total data for PRNN are displayed in Figure 9 and Figure 10, respectively, show a perfect classification of 15 RB and 19 BB signals from the given dataset. The best validation performance is obtained at the 23rd epoch in 0.07s with a loss function value of 5.22 x 10^{-6}. As is evident from Figure 10, AUC has a value of 1 for all the datasets, which shows the maximum distinguishability between the classes. The 100% accuracy, sensitivity, specificity, and precision shown by supervised learning techniques suggest that the non-linear measures are the better choice for classifying RB and BB signals. The proposed method using the PSD and the non-linear time-series features suggests an improved prediction accuracy (86.5% and 100.00%) than the above-discussed machine learning architectures in classifying normal (BB) and adventitious (RB) lung sounds.

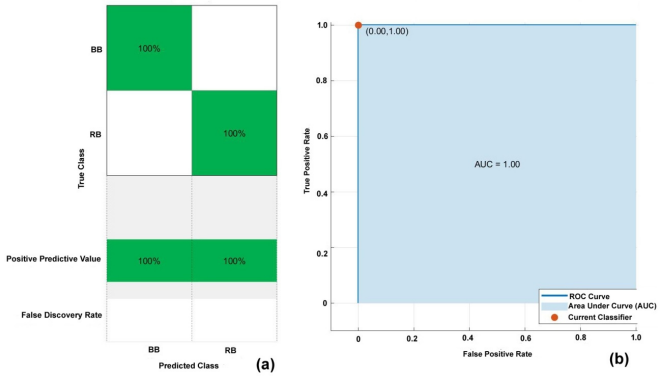

Fig 7. (a) Confusion matrix derived from LDA classifier showing the prediction accuracy of BB and RB and (b) corresponding AUC derived from the LDA classifier for BB and RB.

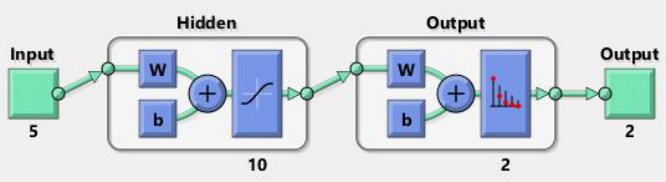

Fig 8. The PRNN structure.

4 Conclusion

The work elucidated in the paper is a stepping stone in the development of a potential tool for pulmonary auscultations using non-linear measures-based classification. The signals are analyzed by employing mathematical techniques like fast Fourier transform, time-frequency localization using wavelet, phase portrait, non-linear time-series, fractal, and machine learning techniques. It is reported that the novel coronavirus also affects the lungs and respiratory tract, causing short-term or acute bronchitis symptoms, which suggests the possibility of extending these techniques to COVID – 19 auscultations. The analysis of thirty-four samples both in time and frequency domains unveils a lesser number of component frequencies, and its overtones of lower intensities in the RB signal help in distinguishing RB from BB. The wavelet scalogram displays the characteristic features of RB, like longer respiration time, lesser frequency spread, and sequential intermittent damping oscillations. The dynamics of airflow during RB and BB up on analyzing by fractal and time-series analyses reveal the complexity involved. The persistence of intense multiple frequency components, seen in the spectral density plot and wavelet scalogram of BB, reveals the same higher

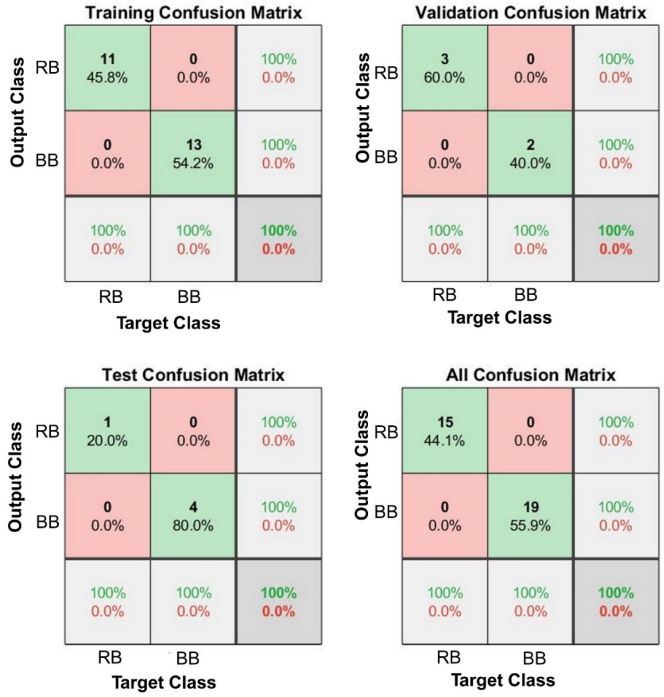

Fig 9. Confusion matrices for training, validation, testing, and prediction of BB and RB.

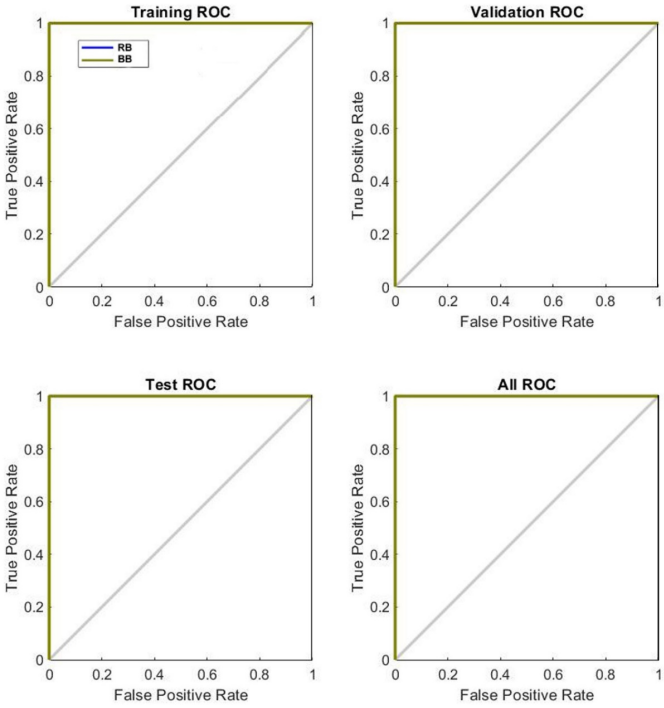

Fig 10. AUC derived from pattern recognition for BB and RB signals.

complexity as observed in the fractal analysis. The value of the Hurst exponent, though, suggests both RB and BB signals to be antipersistent; its higher value for RB indicates the randomness involved in the airflow dynamics through the air passage in the lungs. The maximal Lyapunov exponent, as well as the phase portrait, reveal the complexity of the system. The higher entropy value of the RB signal, besides depicting the complexity of airflow, gives information about the internal morphology of the airways containing mucus and other obstructions. When the features extracted from power spectral data detail the signal magnitude, the non-linear measures - S, λ, m, D, and τ – tell the temporal correlation of the data points that represents the signal's multidimensional properties such as complexity and randomness. The unsupervised classifier PCA using the features extracted from PSD data helps in distinguishing RB from BB, with a total variance of 86.5%. The supervised learning models - LDA and PRNN - employing non-linear time-series parameters help not only in classifying the RB and BB signals but also in predicting them with 100% accuracy, sensitivity, specificity, and precision.

5 Author Contributions

All the authors have equally contributed to this work.

References

1) Jung SY, Liao CH, Wu YS, Yuan SM, Sun CT. Efficiently Classifying Lung Sounds through Depthwise Separable CNN Models with Fused STFT and MFCC Features. *Diagnostics*. 2021;11(4):732–732. Available from: https://doi.org/10.3390/diagnostics11040732.
2) Feng Y, Wang Y, Zeng C, Mao H. Artificial Intelligence and Machine Learning in Chronic Airway Diseases: Focus on Asthma and Chronic Obstructive Pulmonary Disease. *International Journal of Medical Sciences*. 2021;18(13):2871–2889.
3) Rao A, Huynh E, Royston TJ, Kornblith A, Roy S. Acoustic Methods for Pulmonary Diagnosis. *IEEE Reviews in Biomedical Engineering*. 2019;12:221–239. doi:10.1109/RBME.2018.2874353.
4) Wang Z, Chen X, Lu Y, Chen F, Zhang W. Clinical characteristics and therapeutic procedure for four cases with 2019 novel coronavirus pneumonia receiving combined Chinese and Western medicine treatment. *BioScience Trends*. 2020;14(1):64–68. doi:10.5582/bst.2020.01030.
5) Kim Y, Hyon Y, Jung SS, Lee S, Yoo G, Chung C, et al. Respiratory sound classification for crackles, wheezes, and rhonchi in the clinical field using deep learning. *Scientific Reports*. 2021;11(1):1–11. Available from: https://doi.org/10.1038/s41598-021-96724-7.
6) Pal R, Barney A. Iterative envelope mean fractal dimension filter for the separation of crackles from normal breath sounds. *Biomedical Signal Processing and Control*. 2021;66:102454–102454. Available from: https://doi.org/10.1016/j.bspc.2021.102454.
7) Swapna MS, Renjini A, Raj V, Sreejyothi S, Sankararaman S. Time series and fractal analyses of wheezing: a novel approach. *Physical and Engineering Sciences in Medicine*. 2020. Available from: http://link.springer.com/10.1007/s13246-020-00937-5.
8) Raj V, Renjini A, Swapna MS, Sreejyothi S, Sankararaman S. Nonlinear time series and principal component analyses: Potential diagnostic tools for COVID-19 auscultation. *Chaos, Solitons & Fractals*. 2020;140:110246–110246. doi:10.1016/j.chaos.2020.110246.
9) Sankararaman S. Unveiling the potential of phase portrait-based recurrence network: a revelation through lung sound analysis. *Journal of Complex Networks*. 2021;10(1):46–46. Available from: https://doi.org/10.1093/comnet/cnab046.
10) Komalasari R, Rizal A, Suratman FY. Classification of Normal and Murmur Hearts Sound using the Fractal Method. *International Journal of Advanced Trends in Computer Science and Engineering*. 2020;9(5):8178–8183. Available from: https://doi.org/10.30534/ijatcse/2020/181952020.
11) Nguyen QN, Liu AB, Lin CW. Development of a Neurodegenerative Disease Gait Classification Algorithm Using Multiscale Sample Entropy and Machine Learning Classifiers. *Entropy*. 2020;22(12):1340–1340. Available from: https://www.mdpi.com/1099-4300/22/12/1340.
12) Erickson B, Wrigley D, French W, O'Brien T. Easyauscultation. 2021. Available from: https://www.easyauscultation.com/cases?coursecaseorder=1&courseid=201.
13) Medzcool, Gassner B, Selbak R. Rhonchi Lung Sounds. 2019. Available from: https://youtu.be/YgDiMpCZo0w.
14) Williams S, Gassner B, Selbak R. Lung Sounds Collection. 2020. Available from: https://emtprep.com/free-training/video/lung-sounds-collection.
15) Osgood BG. Lectures on the Fourier Transform and its Applications. Rhode Island, USA. American Mathematical Society. 2019.
16) Rhif M, Abbes AB, Farah I, Martínez BR, Sang Y. Wavelet Transform Application for/in Non-Stationary Time-Series Analysis: A Review. *Applied Sciences*. 2019;9(7):1345–1345. Available from: https://doi.org/10.3390/app9071345.
17) De Las NLGM, Requena J. Different methodologies and uses of the Hurst exponent in econophysics. *Studies of Applied Economics*. 2019;37(2):1–13.
18) Zhang Q, Ding J, Kong W, Liu Y, Wang Q, Jiang T. Epilepsy prediction through optimized multidimensional sample entropy and Bi-LSTM. *Biomedical Signal Processing and Control*. 2021;64:102293–102293.
19) Chen C, Sun S, Cao Z, Shi Y, Sun B, Zhang XD. A comprehensive comparison and overview of R packages for calculating sample entropy. *Biology Methods and Protocols*. 2019;4(1). doi:10.1093/biomethods/bpz016.
20) Kulkarni A, Chong D, Batarseh FA. Foundations of data imbalance and solutions for a data democracy. *Data Democracy*. 2020;2020:83–106. Available from: https://linkinghub.elsevier.com/retrieve/pii/B9780128183663000058.
21) Baghel N, Nangia V, Dutta MK. ALSD-Net: Automatic lung sounds diagnosis network from pulmonary signals. *Neural Computing and Applications*. 2021;33(24):17103–17118. Available from: https://doi.org/10.1007/s00521-021-06302-1.
22) Hasan B, Abdulazeez AM. A review of principal component analysis algorithm for dimensionality reduction. *Journal of Soft Computing and Data Mining*. 2021;2(1):20–30.
23) Hassan M, Ali S, Alquhayz H, Safdar K. Developing intelligent medical image modality classification system using deep transfer learning and LDA. *Scientific Reports*. 2020;10(1):1–14.
24) Abdullah MK. Diagnosis on lung cancer using artificial neural network. Fen Bilimleri Enstitüsü. 2019.